Quantification of the surface porosity in high burn-up fuel using image analysis tools

D. Gavillet

Division Hot Laboratory (AHL), Nuclear Energy and Safety Department
Paul Scherrer Institut, Switzerland

(Proceeding of the 45th annual meeting "Hot laboratories and remote handling' working group; Kendal, England, 22-23 September 2008

Abstract

The size and number density of the pores in high burn-up fuel are key parameters for the modelling of the fission gas distribution and release. This study is an attempt to determine the porosity parameters (size and number density) using Optical Microscopy images and Secondary Electron images acquired on cross sections of high burn-up fuel.

The images were collected during the Post Irradiation Examination of a Pressure water Reactor fuel rod irradiated to an average burn-up of about 105 GWd/tHM. They have been analysed using commercial image analysis software (AnalySIS®) allowing the determination of the main characteristics of the distribution of pores or particles exhibiting a well defined colour contrast variation with their surroundings. The original images used in this study were extracted from a standard Post Irradiation Examination work without specific contrast enhancements that would improve the image analysis procedure.

The influence of different parameters like the magnification of the images and the type of images used are studied in order to determine the necessary conditions for a good determination of the porosity with this method.

This study proves that such an analysis delivers reliable data only if realised on high magnification pictures acquired in such conditions that the pore contrasts are specifically enhanced for further image analysis.

1 Introduction

As a result of the fission process in nuclear fuel, gases are formed. The so called Fission Gas (FG) atoms can be dissolved in the fuel matrix or precipitated in nm-sized intra-granular bubbles within the fuel grain, in μm-sized intergranular bubbles at the grain boundaries, and in μm-sized pores resulting from the fuel production process. A fraction of the FG can be released into the plenum or the fuel-cladding gap of the nuclear fuel rod increasing its inner pressure. However a large amount is still trapped in the bubbles or pores inside the fuel. The local temperature, the fuel type and the local burnup are the main parameters determining the exact distribution of the FG.

The presence of μm-sized bubble and -pore containing pressurized fission gases has to be considered for fuel performances at increasing burn-ups. Especially for possible accidents, like loss of coolant accident (LOCA) or reactivity initiated accident (RIA), the behaviour of the gases has to be considered. The knowledge of the distribution and location of the FG Xe and Kr in irradiated nuclear fuel is therefore of major interest. In order to make fine analyses of the Fission Gas Release (FGR) under steady-state and transient conditions, there is a high demand on the knowledge on the FG inventory in the fuel, especially in the μm-sized inter-granular bubbles and in the fine porosity created in the High Burnup Structure (HBS) at the periphery of the pellet. Thus, quantitative analyses of FG in nuclear fuel are required and prerequisite for fuel behaviour prediction under accident conditions. In particular the quantitative measurement of the local FG inventory in the fuel requests a detailed knowledge of the pore size distribution and density.

This study is an attempt to use image analysis for the detailed characterisation of the local pore size and density in high burn-up fuel. These parameters are a key information for the quantification of experimental measurement of fission gas concentration in the fuel and therefore for the validation of fission gas release models [1, 2].

Optical (OM) as well as secondary electron (SE) images were collected during the Post Irradiation Examination (PIE) of a Pressure Water Reactor (PWR) fuel rod irradiated to ultra high burn-up (105 GWd/tHM). They were analysed using standard image analysis software delivering the pore size distribution parameters.

This paper describes the data acquisition method and the control procedure used to validate the results.

2 Specimen

The specimen used in this study has been extracted from a PWR UO_2 rod irradiated to an average burnup of 105 GWd/tHM. The local burn-up in the specimen was 120 GWd/tHM. The local burn-up at the periphery of the pellet was experimentally evaluated to be over 300 GWd/tHM.

3 Image collection

The pore size and density analysis has been realised on three sets of pictures collected on the same specimen:

The first set was extracted from the ceramography analysis of the specimen using an optical microscope. The set is composed of images collected along a radius of the pellet cross section at an optical magnification of about 500x. All images have been recorded with a colour digital camera at a resolution of 1300 x 1030 pixels. Typical original images used in this study are presented in Figure 1. The intrinsic spatial resolution of the OM limits the analysis to pores with a diameter larger than few micrometers. In addition, the magnification must be choosing so that the number of pixels per pores is large enough to give a correct size measurement of the pore. In this study, at radius larger than 0.6 R_0, the resolution of the picture is no more good enough in view of the very high density of very small pores. The total surface analysed per frame is about 54'100 μm^2 and the typical number of pores detected per frame is in the range of 400 to 2500 pores.

The second set of images has been collected with a shielded electron microprobe (EPMA) on the same specimen along the same radius as the first set. The magnification of the images is about 600x with a resolution of 512 x 512 pixels. This method allows the analysis of smaller pores than the OM at the condition that the magnification is adapted to the pore size (enough pixel per pores). The contrasts of the SE images were not optimised for the image analysis procedure but for PIE characterisation of the fuel. In particular the relatively large white contrast appearing at one edge of the pores, due to electronic loading, complicates the analysis. Typical original images used in this study are presented in Figure 2. The total surface analysed per frame is usually about 38'000 μm^2 but can be smaller in presence of cracks that are removed from the analysis and the typical number of pores detected per frame is in the range 200 to 1000 pores.

Finally, the third set of images used in this study was high magnification EPMA images (about 2500x; Secondary Electron, 512 x 512 pixels) collected again along the same pellet radius and usually at the same position as the second set. The surface analysed is about 2400 μm^2 and about 40 to 300 pores are detected per frame, resulting in a relatively poor statistic but a very good resolution of the small pores. Typical examples of the analysed images are presented in Figure 3.

Pellet centre	¼ pellet radius (0.25 R_0)	½ pellet radius (0.5 R_0)
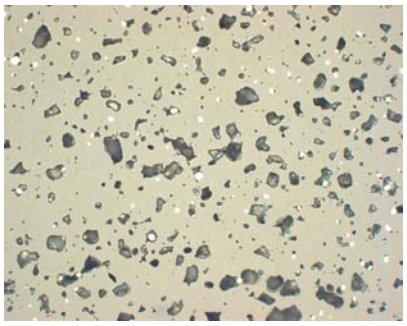	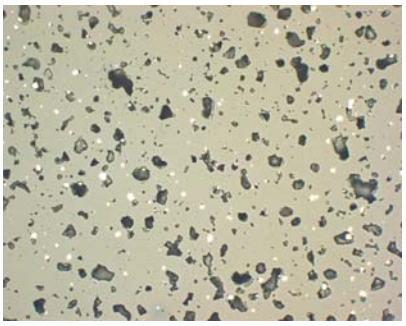	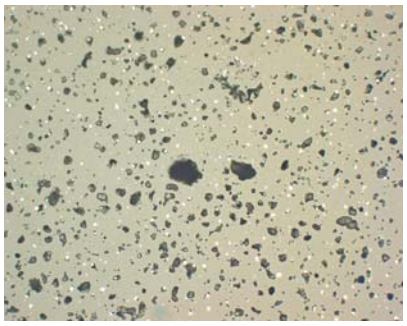

Figure 1 Typical OM-Images used for the image analysis in this study. The full width of the picture corresponds to 261 μm (set 1).

Pellet centre (0.06 R_0)	½ pellet radius (0.52 R_0)	Pellet periphery (0.95 – 1 R_0)
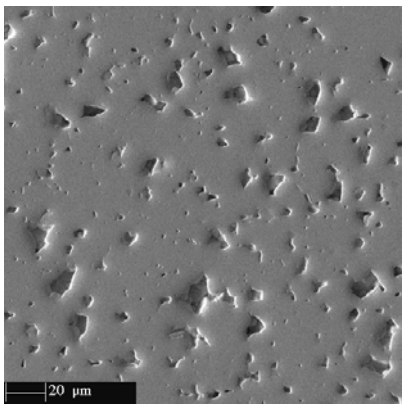	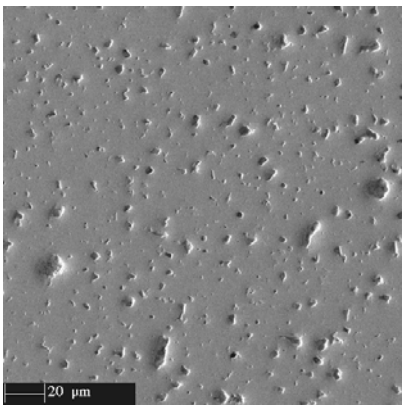	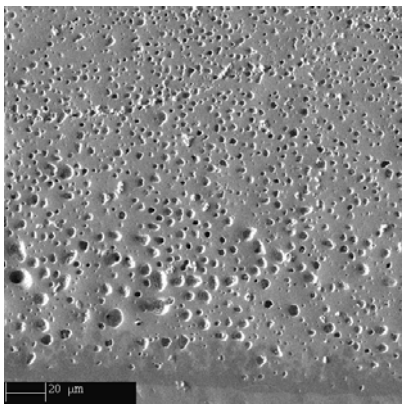

Figure 2 Typical SE-images used for the image analysis in this study (set 2)

Pellet centre (0.06 R_0)	½ pellet radius (0.52 R_0)	pellet periphery (0.98 R_0)
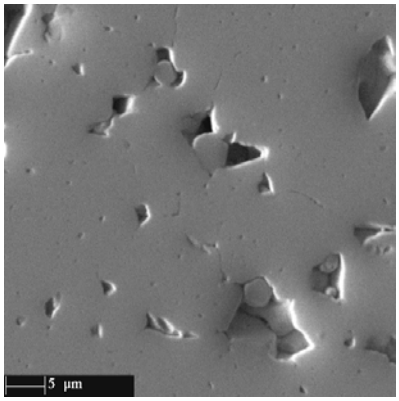	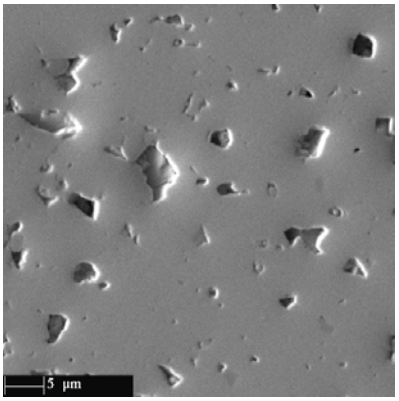	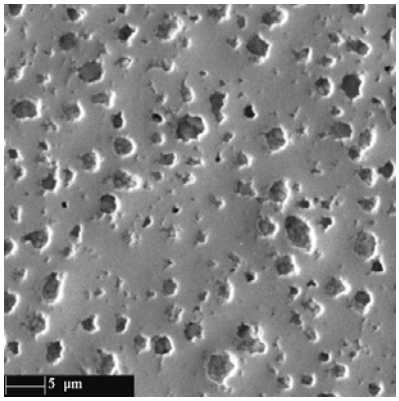

Figure 3 Typical examples of the high magnification SE images (set 3).

4 Image analysis method

The image analysis has been realised with the commercially available software AnalySIS™ 3.1. The original colour images are first converted in grey coded black and white images. The contrasts are slightly enhanced and the image is converted in a binary image using operator adjusted thresholds. Then the binary image is cleaned with morphological

filters in order to remove the background noise (Erosion) and fill up the pores (Dilatation). A ***frame*** is then set defining the zone to be analysed on the picture. Finally, the software delivers different morphological parameters of all detected pores in the frame. In this study the following parameters have been recorded: the ***Fractional Porosity*** (FP) corresponding to the surface fraction of all pore related to the analysed frame surface in %, the ***Pore Density*** (PD) corresponding to the number of pores detected per surface unit in the frame and the pore ***Equivalent Circular Diameter*** (ECD) corresponding to the diameter of a circle having the same surface as the measured pore. The ***Pore Size Distribution*** (PSD), corresponding to the variation of the number of pore in size classes, is calculated using the ECD of all pores detected. Finally the ***average ECD*** is the arithmetic average of all pores ECD measured in the frame.

Two steps of this procedure, the threshold setting for the binarisation and the cleaning procedure are clearly operator dependant and must be adjusted on all pictures in function of the local contrast and pore size in the analysed zone.

In order to determine standard parameters for a set of images, reference images are needed. Such reference images were created by binarising some of the images of each set manually by painting the pores. This method creates a very good representation of the real pore structure and allows eliminating most of the artefacts present in the pictures. Since the generated drawings are basically binary images, they are intrinsically insensitive to any threshold setting and do not need any cleaning procedure. Typical examples for the three sets of images are given in Figure 4.

5 Sensitivity study

In order to determine the sensitivity of the analysis method to the threshold and cleaning procedure, a series of analysis was made using different settings.

First a standard procedure has been developed in order to get a semi-automatic procedure applicable to all pictures of a set using the same threshold setting and cleaning procedure. The standard procedure is then validated by comparing the results obtained with data extracted from the reference images.

The sensitivity study has been realised by the binarisation of images using varying threshold settings (T1, T2, T3, …) in order to record the resulting effect on the porosity parameters (FP, ECD, PSD). The results of the sensitivity analysis of one image of set 1 are presented in Figure 5, Table 1 and Figure 6.

Similar analyses have been realised on the second set of image (SE – low magnification). The values of the FP and ECD resulting from the different settings on one picture are presented in Table 2.

The complete analysis demonstrates that the fractional porosity (FP) and the number of pores detected per frame are very sensitive to the threshold settings but the shape of the pore size distribution (PSD) and average equivalent circular diameter (ECD) are quite insensitive (Example in Figure 6, Table 1 and Table 2).

A detailed evaluation shows that the sensitivity is very large on OM pictures with high density of small pores ($R > 0.5R_0$) for both the fractional porosity and the number of pores detected. This is clearly linked to the limited resolution of the image and the high density of the pores. A small variation of the threshold produces a relatively large variation of the surface recognised as pore and the filtering can remove a large number of small pores. These images are then clearly not appropriate for such analysis.

On the SE images, the number of pores detected is less sensitive to the threshold setting and filtering procedure than on the OM images, but the fractional porosity is sensitive because of the relatively weak contrast variation between the pore interior and the polished fuel surface as well as the difficulty to account for the pore edge contrast (electron charging).

This is particularly evident in the analysis of the images at the pellet centre. It appears also that the magnification chosen is not large enough for the analysis of the fine porosity.

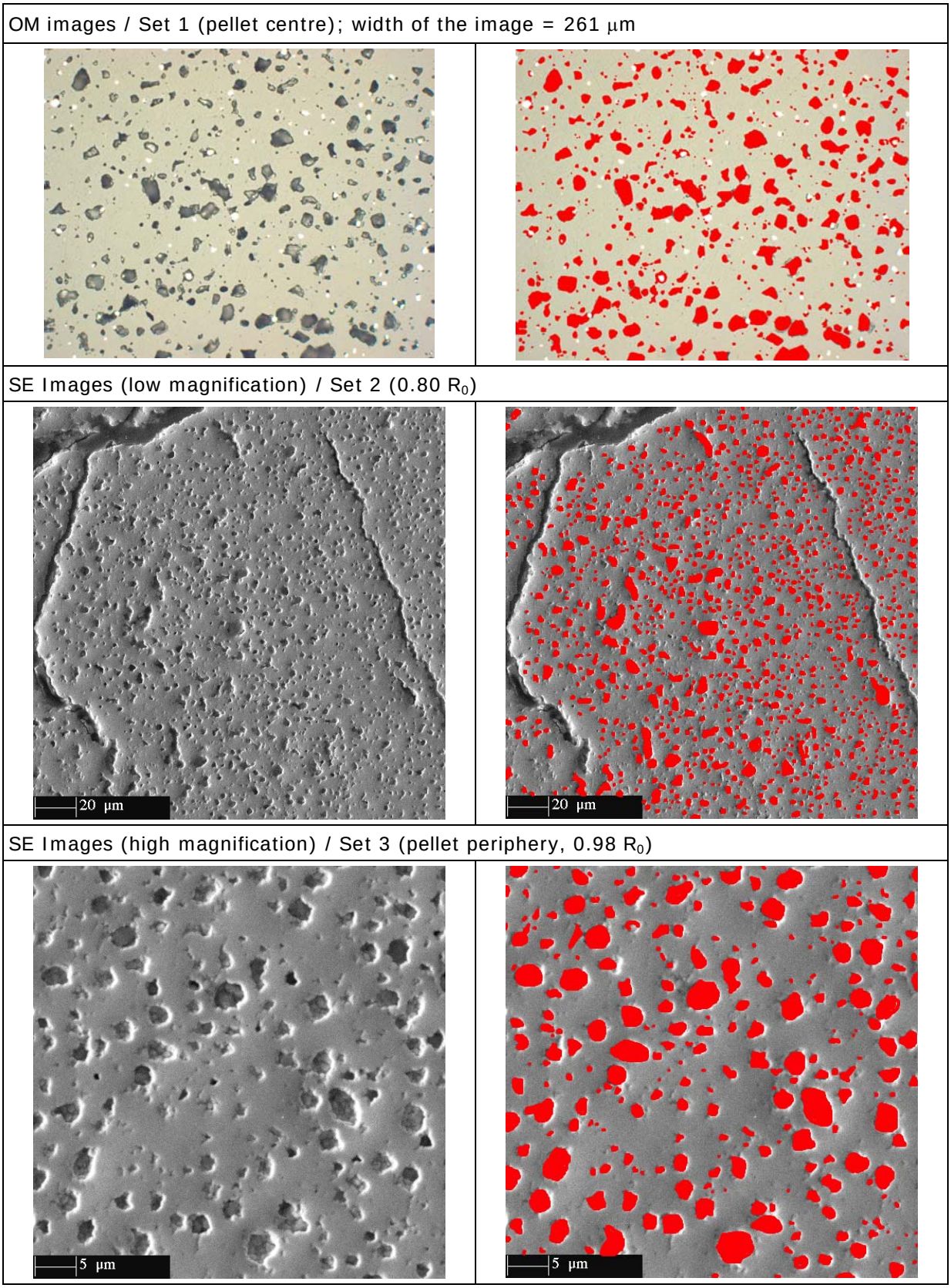

Figure 4 Typical examples of the manual binarisation of images for the three sets used in this study (left original images and right images with manually painted pores.

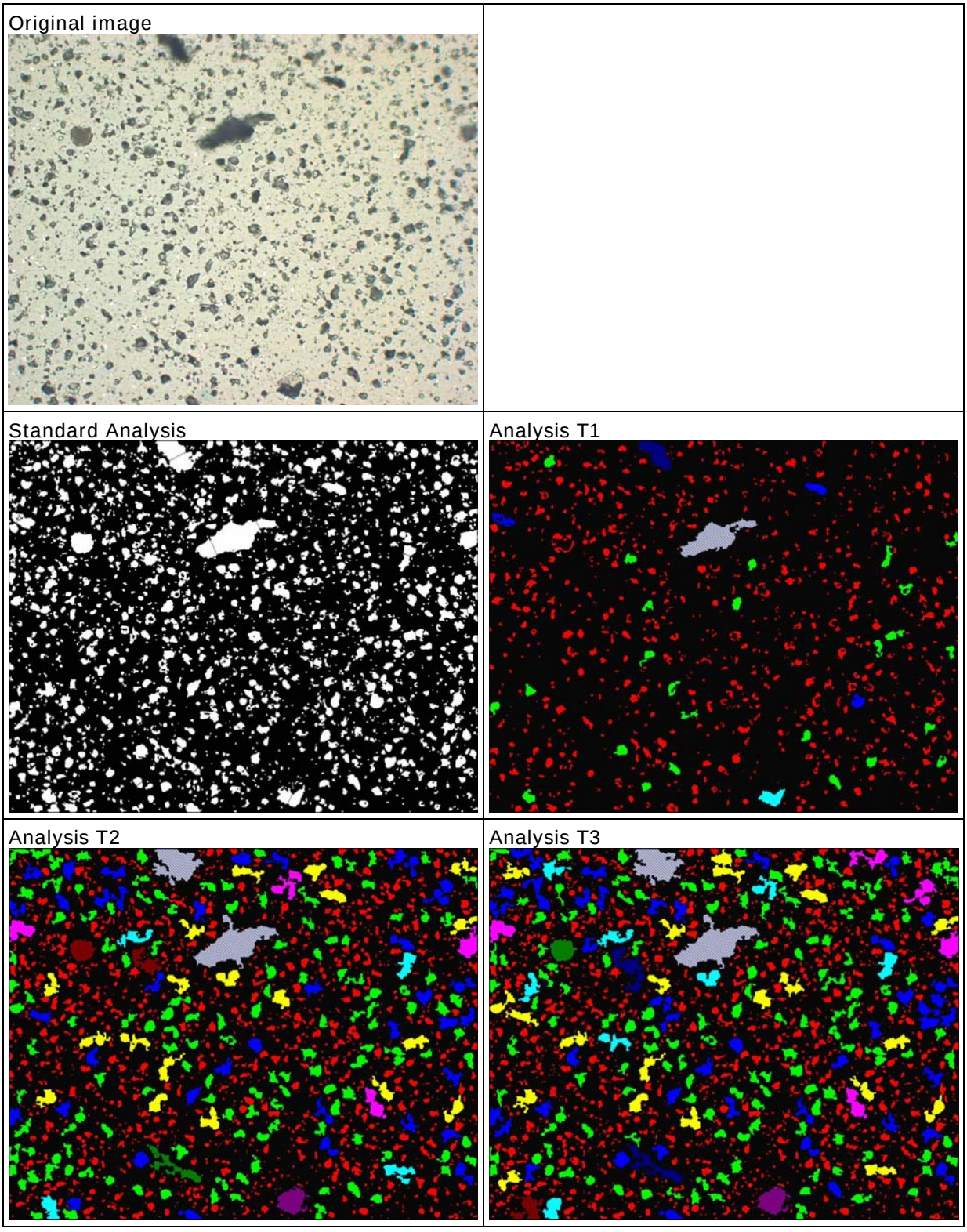

Figure 5 Original image and pore analysis results from the sensitivity analysis on a picture of set 1 (OM) at pellet mid radius. The pore size is colour coded. T1, T2 and T3 are corresponding to different threshold settings. The full width of the picture corresponds to 261 μm.

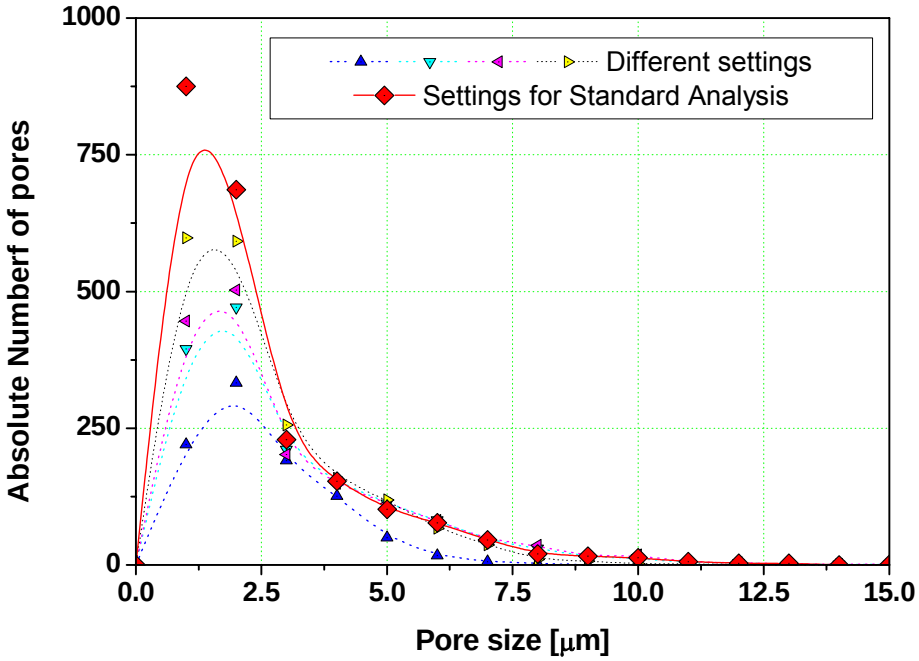

Figure 6 Pore Equivalent Diameter (ECD) distribution obtained with the different analysis procedures (T1 to T4) on an OM-picture at pellet mid radius.

Table 1 Pore distribution parameters obtained with the different analysis procedures on a OM-picture at the pellet centre.

Analysis	Total surface analysed (μm^2)	Fractional porosity (%)	No. of pores detected	Average. ECD (μm)
Standard	54097	19.9	1852	2.1
T1	54097	9.0	949	2.1
T2	54097	25.3	1539	2.5
T3	54097	27.4	1624	2.5

Table 2 Pore distribution parameters obtained with the different analysis procedures on a SE-picture acquired at $0.8R_0$.

Analysis	Total surface analysed (μm^2)	Fractional porosity (%)	No. of pores detected	Average. ECD (μm)
Standard	38019	16.7	811	2.7
T1	29931	14.9	646	2.6
T2	30136	15.0	643	2.6
T3	29451	10.8	556	2.4

6 Validation of the results

The standard procedure defined in the sensitivity study has been used to get the local porosity characteristics along a radius of the pellet with set 1 and set 2. Simultaneously, the reference images have been analysed and the results are compared.

The results are presented in Figure 7. This confirms the problems recognised in the sensitivity study. If the average pore size (average ECD) as well as the pore size distribution (PSD, not shown here) are acceptably determined, at least in the centre of the pellet, the fractional porosity but also the pore density are underestimated mostly at the pellet periphery. This seems to be linked to the small size and large density of pores in this zone.

Therefore, it was decided to check the data obtained by analysing SE images acquired at higher magnification (set 3). In order to get a very good data set for this check, the images have been manually digitised like for the reference images of the set 1 and 2.

The analysis demonstrates that if the overall variations of the pore size (PSD), pore density (PD) and fractional porosity (FP) are similar when extracted from high resolution images, the obtained absolute values are very different. The fractional porosity is basically the same, but the pore density is much larger mostly at the pellet periphery and the average pore size is much smaller at all radii (Figure 8).

In addition, in spite of the low statistics, the shape of the pore size distribution is basically identical to the one obtained on the previous analysis (not shown here).

This confirms the analysis realised in the precedent paragraphs. It shows that the fine porosity is not well recorded by the analysis of relatively low magnification images but that the fractional porosity is correctly evaluated as the small pores do not contribute significantly to this parameter.

It is concluded that the porosity parameters generated from the high resolution SE images are the most precise in spite of the low statistics. Some more frame analyses in the periphery and in the pellet centre would improve even more the quality of the data set.

7 Discussion and comparison with published analysis

In order to back up the assumption that the best data set of this study has been obtained with the image set 3, the results are compared with published values for fuel irradiated to a lower rod average burn-up (80 and 98 GWd/tHM; [4, 5]) under the same conditions (Figure 9).

The values obtained for the analysis of the high magnification SE images are in good agreement with the data published by Spino et al. The difference can be easily explained by the burn-up difference between the two data sets.

In comparison to the lower burn-up observation a slightly higher fractional porosity is observed in the centre of the pellet as well as at the periphery of the pellet from a radius of about 0.7 R_0. This result suggests that the amount of restructured fuel has increased with the burn-up in this zone but that the zone has not extended toward the centre of the pellet. The strong increase of the porosity at the edge of the pellet with the burn-up is also confirmed by the present study.

In the centre of the pellet a slightly higher average pore size but a slightly lower pore density are observed. This could indicate that some pore growth has occurred in this region. From mid radius to pellet edge no variation of the average pore size in function of the burn-up is observed but an increase of the pore density indicating that the increase of porosity results from the formation of new pores. The decrease of the pore density and increase of the pore size at the pellet periphery (100 μm at pellet periphery) is also confirmed in this study.

Due to the specimen preparation procedure a small enlargement of the pores can be expected. This would induce a systematic error in the porosity characteristics (overestimation of the average pore size and of the fractional porosity). As the specimen preparation is similar in the present study and in the one published by Spino et al., this effect is expected to be similar in both studies.

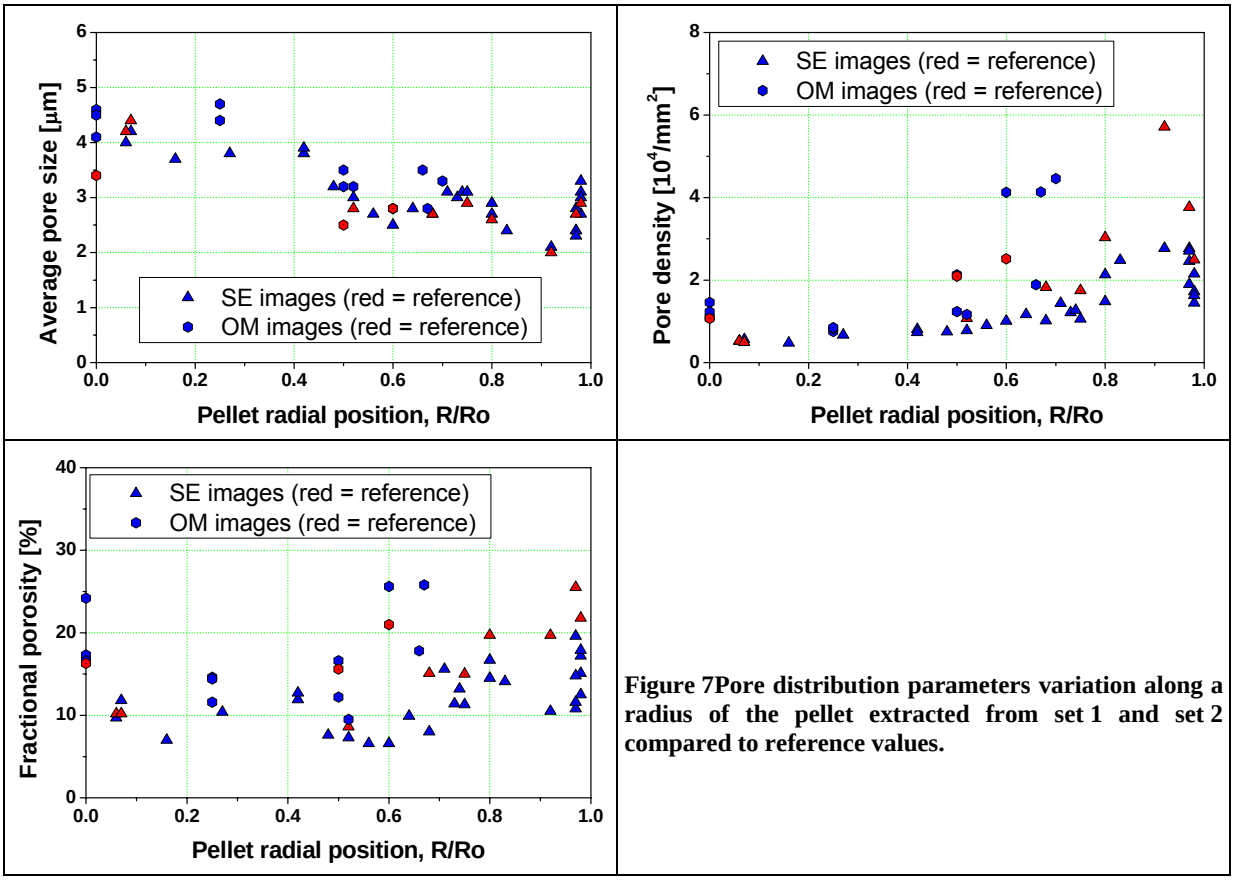

Figure 7Pore distribution parameters variation along a radius of the pellet extracted from set 1 and set 2 compared to reference values.

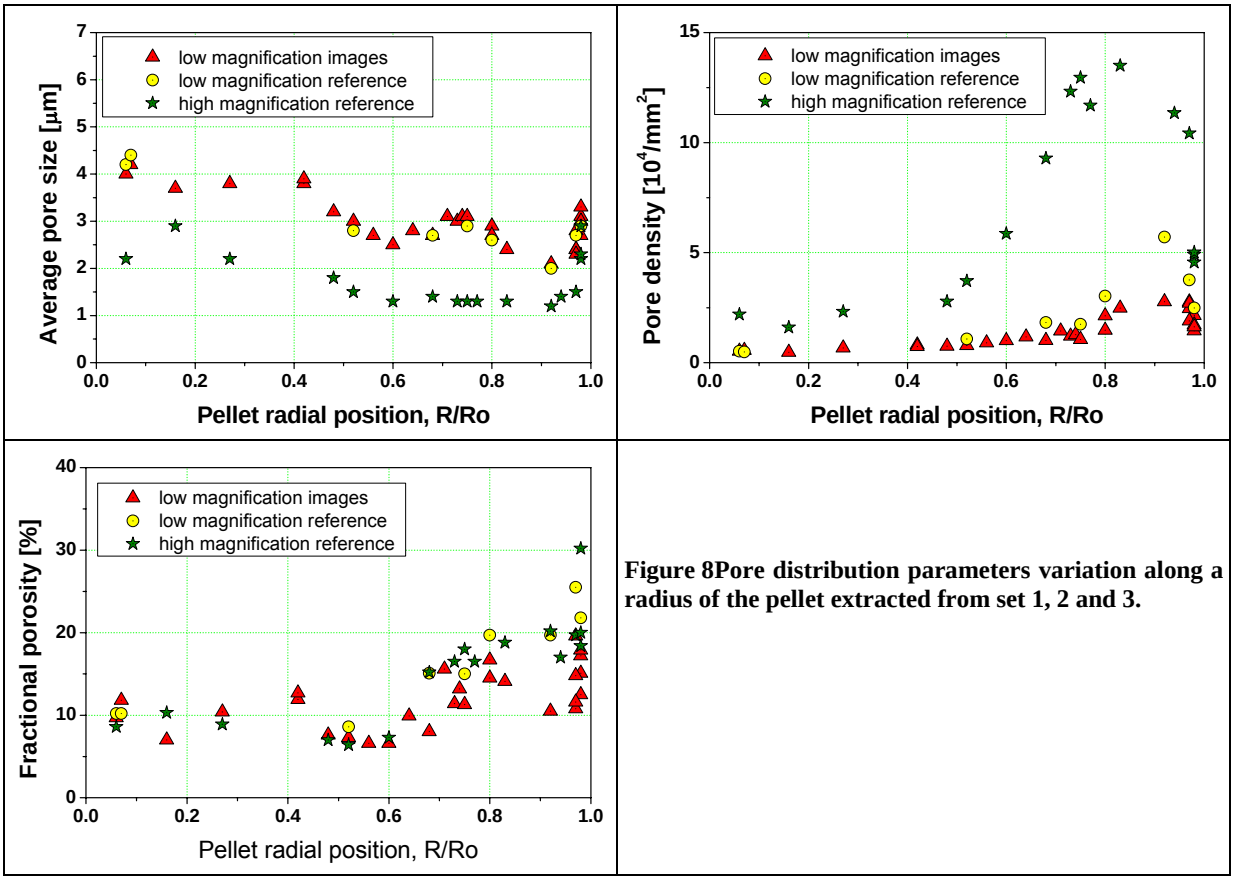

Figure 8Pore distribution parameters variation along a radius of the pellet extracted from set 1, 2 and 3.

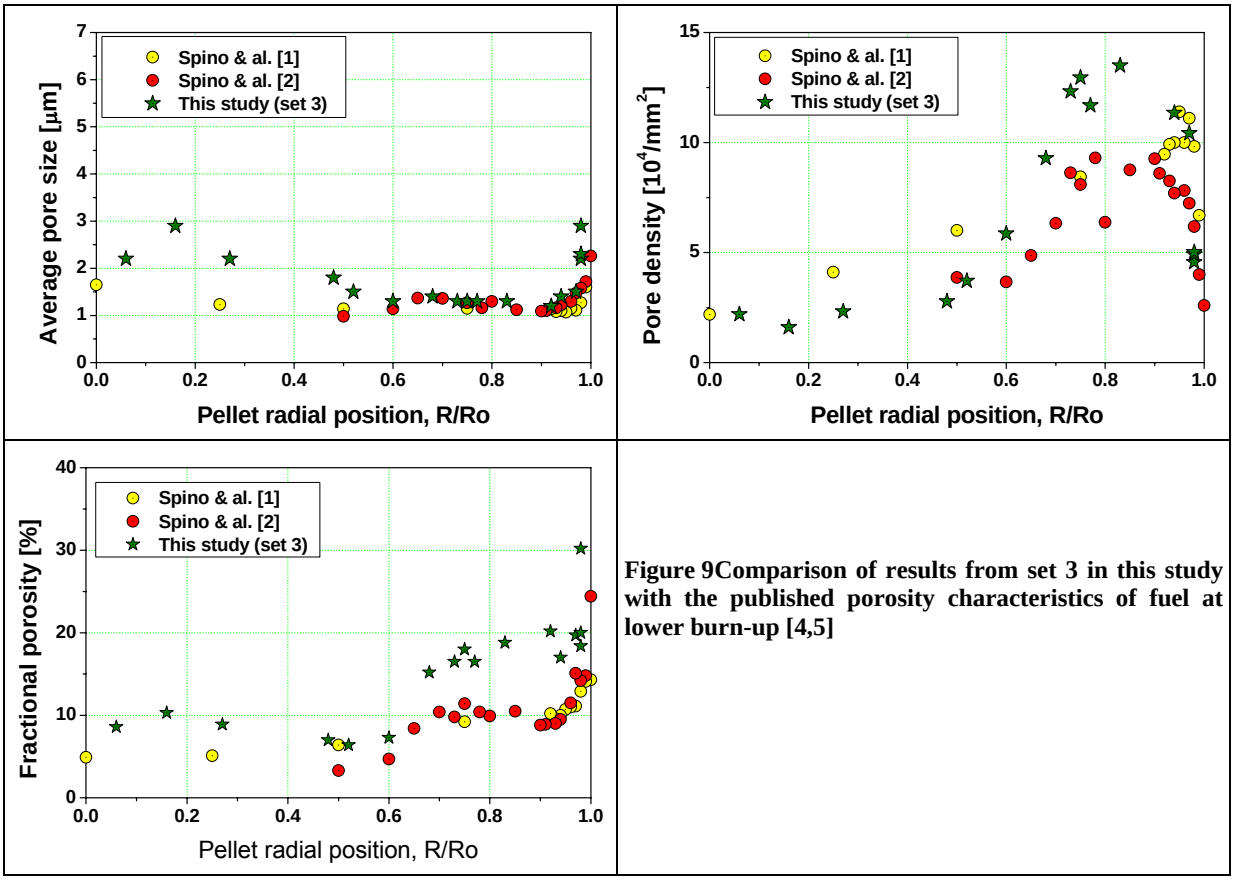

Figure 9Comparison of results from set 3 in this study with the published porosity characteristics of fuel at lower burn-up [4,5]

8 Conclusion

Optical Microscopy images and Secondary Electron images realised during the Post Irradiation Examination of cross sections of very high burn-up fuel rod (105 GWd/tHM rod average) were used for the analysis of the porosity characteristics in the pellet.

The detailed study has demonstrated that the choice of magnification of the images used in such a study is critical in order to obtain a good determination of the porosity parameters. It also shows that the acquisition of the images in future studies must be specifically optimised to get good contrasts of the pore edges. This would allow an easy and fast semi-automatic image analysis of a large number of frames insuring a good statistics in the parameter determination.

With this study, on non-optimised images, good data have been obtained on high magnification SE images binarised manually at the cost of a poor statistics.

The analysis confirms the trends observed by Spino et al. [4, 5] in fuel irradiated at lower burn-up in the same reactor.

9 Acknowledgement

The author would like to acknowledge the contribution of R. Restani and A. Urech who realised the EPMA and the ceramography analyses respectively and produced all pictures used in this study. Also, R. Brütsch has been very helpfull for the definition of the image analysis procedure used in this study.

Finally I. Günther-Leopold has greatly contributed to improve the paper by her critical review and numerous comments.

10 References

[1] M. Horvath, M. Guillong, A. Izmer, N. Kivel, R. Restani, I. Günther-Leopold, J. Opitz Coutureau, Ch. Hellwig and D. Günther; “Analysis of Xenon gas inclusions in nuclear fuel using laser ablation ICP-MS”; J. Analytical Atomic Spectrometry, 2007 22(10), 1266-1274

[2] A. Romano, M.I. Horvath and R. Restani; “Evolution of porosity in the high burnup fuel structure” J. of Nucl. Mat. 361 (2007) 62-68

[3] Ch. Hellwig, M.I. Horvath, P. R. Blair, R. Chawla and D. Günther; “Fission Gas Distribution and Behavior in the High burn-up Structure”; Proceding of the 2007 Int. LWR Fuel Performance Meeting, Oct. 2007, paper 1029, San Francisco

[4] J. Spino, K. Vennix, M. Coquerelle; “Detailed characterisation of the rim microstructure in PWR fuels in the burn-up range 40-67 GWd/tM”; Journal of Nuclear Material 231 (1996) 179-190

[5] J. Spino, A.D. Stalios, H. Santa Cruz, D. Baron; “Stereological evolution of the rim structure in PWR-fuels at prolonged irradiation: Dependencies with burn-up and temperature”; Journal of Nuclear Material 354 (2006) 66-84